THE JOURNAL OF PHYSICAL CHEMISTRY B

Article

pubs.acs.org/JPCB

Adsorption from Binary Solutions on the Polymer-Tethered Surfaces

M. Borówko, S. Sokołowski, and T. Staszewski*

Department for the Modeling of Physico-Chemical Processes, Maria Curie-Skłodowska University, 20-031 Lublin, Poland

ABSTRACT: A density functional study of adsorption from binary solutions on surfaces modified with tethered chains is presented. The tethered chains are modeled as freely jointed tangent spheres. The fluid molecules are spherical. All species interact via the Lennard-Jones (12−6) potential. The substrate is neutral with respect to all chain segments but the surface-binding segment, and it interacts with the fluid molecules via a Lennard-Jones (9−3) potential. Depending on the parameters of the model, different shapes of the relative excess adsorption isotherms are found. The density profiles of all components are analyzed. It is shown that the surface region is highly inhomogeneous. An influence of the grafting density, the length of grafted chains, the nature of the solution, and its composition on the adsorption mechanism and the structure of the bonded-phase is investigated. The theoretical predictions are consistent with the results of computer simulations and experimental data.

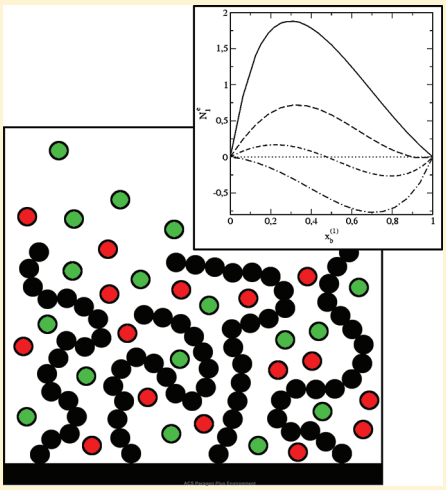

1. INTRODUCTION

Adsorption from solutions on polymer-tethered surfaces plays an important role in a variety of biological and physicochemical processes. One of significant applications of this phenomenon is the separation of sample components in reversed-phase liquid chromatography (RPLC). As it has been already estimated, about 90% of analytical separations of small molecules are performed using this technique.[1,2]

The essence of chromatography is that a flow of a mobile phase causes a differentiated migration of sample components along the chromatographic bed. The aim is to achieve a good separation of all sample components in a reasonable time. The choice of the optimal conditions for the separation is a difficult task because the process depends, in a very complicated way, on properties of the stationary and liquid phases. In the RPLC, the silica gel modified with end-grafted alkyl chains (C_2, C_8, C_{18}, and C_{30}, where the subscript indicates the number of carbon atoms) is used for the packing of chromatographic columns, and aqueous solutions of popular organic solvents (methanol, acetonotrile, tetrahydrofuran) are applied as mobile phases. It is known that a good tool for controlling the separation is a change of the composition of the mobile phase. Much effort has been directed toward the theoretical prediction of the solute retention as a function of the mobile-phase composition.[1−8,10] The theories have been usually based on the lattice model of solutions.[1−4,7,9] The important topic of the study was the mechanism of retention. Two retention models have been usually considered, adsorption at the stationary/mobile phase interface and partitioning between these phases. The question to what extent adsorption and partitioning contribute to the total retention still remains without a full answer. However, it is generally held that interactions between components of the mobile phase and the bonded phase affect considerably this process.

Numerous experimental results of connecting with adsorption from solution on the chemically bonded phases have been published recently.[10−16] On the other hand, in the literature, one can find only a few theoretical works devoted to this problem.[10,11] The bonded phases have been often treated as "usual solid" adsorbents, and theory of adsorption from solutions on solid surfaces[17,18] has been employed to interpret the experimental data. Gritti and Gouichon[11] have used the so-called bi-Langmuir equation for the description of adsorption on the modified surfaces. They have assumed that the adsorbent can be treated as composed of two distinct patches, one representing the surface covered by grafted chains and the second the bare surface of the solid. Although their approach was originally proposed for silica gels modified with trimethylsilane groups (C_1), it has been also used to describe adsorption on brushes built of longer chains.[14−16] However, the phenomenological approach of Gritti and Gouichon[11] does not give any insight into its influence on adsorption of mixture components.

The effects of the brush structure on the solute retention and adsorption of solvents have been investigated using computer simulations.[19−35] The molecular-level modeling gives a deeper insight into the adsorption mechanism. According to simulation results, the properties of the stationary phase, such as the grafting density and chain length, play a key role in the process. The influence of a type of liquid phase and its composition on

Received: January 4, 2012
Revised: February 10, 2012
Published: February 17, 2012

dx.doi.org/10.1021/jp300114y | J. Phys. Chem. B 2012, 116, 3115−3124

retention has also been investigated. It has been shown that the structure of the surface layer depends considerably on the nature of the mixed solvent.

For many years, the grafted polymer layers have been the topic of advanced theoretical considerations. The studies included scaling theories,[36,37] self-consistent field methods,[38−42] single-chain mean-field methods,[43−45] and density functional theories.[46−54] As in the case of molecular simulation studies, the main focus has been paid to the structure of the surface layers. Theoretical studies of adsorption of various molecules on modified adsorbents have received less attention.[50−55] In particular, the competitive adsorption from liquid mixtures has not been investigated using these methods.

In this paper, we use density functional theory to study adsorption of binary liquid mixtures (solutions) of spherical molecules on chemically bonded phases. The theory allows us to obtain quantitative dependencies between adsorption and various parameters characterizing the system. In particular, we can compute excess adsorption and different factors characterizing the fluid structure near the surface. The theoretical calculations need much less computer time than molecular simulations. Because of the aforementioned practical applications, it is interesting to investigate systematically how different parameters affect adsorption. This is a fundamental goal of our work. We want also to check whether the theory employed by us is capable of predicting the general trends observed in the experimental data.

The article is organized as follows. In section 2, we introduce the model and shortly described the computational method. The results are presented in section 3. Finally, we summarize the results and formulate the general conclusions.

2. THEORY

We study adsorption of binary solutions on surfaces modified with end-grafted polymer molecules. To do that, we use the model described in our previous papers.[51−54] The system in question is treated as a ternary mixture in contact with an impenetrable wall. The mixture consists of tethered polymers, P, and spherical molecules of the sort 1 and 2. The grafted molecules are chains built of M tangentially jointed segments. The connectivity of segments belonging to a given molecule is assured by imposing the bonding potential, V_B

$$\exp[-\beta V_B(\mathbf{R})] = \prod_{i=1}^{M-1} \delta(|\mathbf{r}_{i+1} - \mathbf{r}_i| - \sigma^{(P)})/4\pi(\sigma^{(P)})^2 \tag{1}$$

where $\mathbf{R}_k \equiv (\mathbf{r}_1,\mathbf{r}_2,...,\mathbf{r}_M)$ is the vector specifying positions of segments, the symbol δ denotes the Dirac function, $\sigma^{(P)}$ is the polymer segment diameter, and $\beta^{-1} = k_BT$.

All of the spherical species, that is, the segments of chains and molecules 1 and 2, interact via a truncated Lennard-Jones potential

$$u^{(kl)}(r) = \begin{cases} 4\overline{\varepsilon}^{(kl)}[(\sigma^{(kl)}/r)^{12} - (\sigma^{(kl)}/r)^6] & r < r_{cut}^{(kl)} \\ 0 & \text{otherwise} \end{cases} \tag{2}$$

where $\overline{\varepsilon}^{(kl)}$ is the parameter characterizing interactions between species k and l, $\sigma^{(kl)} = 0.5(\sigma^{(k)} + \sigma^{(l)})$ $(k = P, 1, 2)$, r is the distance between interacting spherical segments, and $r_{cut}^{(kl)}$ is the cutoff distance. In our calculations, we assume that $r_{cut}^{(kl)} = 5\sigma^{(kl)}$.

The molecules of the polymer P are irreversibly preadsorbed on the surface. Their first segments are bonded with the substrate by the potential

$$\exp[-\beta v_{s1}^{(P)}(z)] = C\delta(z - \sigma^{(P)}/2) \tag{3}$$

where z is a distance from the surface and C is a constant. The potential 3 implies that the surface-binding segments are located at the distance $z = z_1 = \sigma^{(P)}/2$ from the wall. Although, according to our model, these segments cannot leave the surface, they can move within the xy-plane. In the case of real bonded phases, the surface-binding segments are permanently anchored on the active sites. All of the remaining segments of grafted chains, $i = 2, 3, ..., M$, are "neutral" with respect to the wall, that is, they interact with the surface via the hard-wall potential. In contrast to the neutral segments, the molecules of components 1 and 2 are attracted by the surface, and their interaction with the surface is described by the Lennard-Jones (9−3) potential

$$v^{(k)}(z) = 4\overline{\varepsilon}_s^{(k)}[(z_0^{(k)}/z)^9 - (z_0^{(k)}/z)^3] \tag{4}$$

where $\overline{\varepsilon}_s^{(k)}$ characterizes the strength of interaction between the kth component and the adsorbent $(k = 1, 2)$ and $z_0 = \sigma^{(k)}/2$.

The grafting density, $\rho_P = N_P/A$, where N_P is the number of grafted chains and A denotes the surface area, is fixed. The system is in equilibrium with the reservoir containing only molecules of components 1 and 2. The bulk densities of those species are equal $\rho_b^{(1)}$ and $\rho_b^{(2)}$, respectively.

We use the density functional approach based on the theory originally developed by Yu and Wu.[56−58] This approach has been already used to describe systems involving bonded phases.[48−55] To avoid unnecessary repetition, we outline only the most important steps of the computational procedure.

At the first stage, the free-energy functional is expressed as the sum $F = F_{id} + F_{hs} + F_c + F_{att}$. The ideal part of the free energy, F_{id}, is known exactly.[59] The excess free energy due to hard-sphere interactions, F_{hs}, follows from the fundamental measure theory of Rosenfeld.[60] The chain connectivity contribution, F_c, results from the first-order perturbation theory of Wertheim.[61] These contributions are given by eqs 7, 10, and 12 in ref 54. The attractive interactions between spherical species are described using the mean-field approximation

$$F_{att} = \frac{1}{2}\sum_{k=P,1,2}^{3} \int d\mathbf{r}_1\, d\mathbf{r}_2\, \rho_s^{(k)}(\mathbf{r}_1)\rho_s^{(k)}(\mathbf{r}_2)u^{(kk)}(\mathbf{r}_{12}) + \sum_{k,l=P,1,2;k<l}^{3} \int d\mathbf{r}_1\, d\mathbf{r}_2\, \rho_s^{(k)}(\mathbf{r}_1)\rho_s^{(l)}(\mathbf{r}_2)u^{(kl)}(\mathbf{r}_{12}) \tag{5}$$

where $u_{att}^{(kl)}$ is the attractive part of the Lennard-Jones potential following from the Weeks−Chandler−Anderson scheme[62]

$$u_{att}^{(kl)}(r) = \begin{cases} -\varepsilon^{(kl)} & r < 2^{1/6}\sigma^{(kl)} \\ u^{(kl)}(r) & r \geq 2^{1/6}\sigma^{(kl)} \end{cases} \tag{6}$$

dx.doi.org/10.1021/jp300114y | J. Phys. Chem. B 2012, 116, 3115−3124

and $\rho_s^{(1)} = \rho^{(1)}$ and $\rho_s^{(2)} = \rho^{(2)}$ are the local densities of spherical molecules 1 and 2, whereas $\rho_s^{(P)}$ is the local density of segments of the grafted chains

$$\rho_s^{(P)}(\mathbf{r}) = \sum_{i=1}^{M} \rho_{s,i}^{(P)}(\mathbf{r}) = \sum_{i=1}^{M} \int d\mathbf{R}\, \delta(\mathbf{r} - \mathbf{r}_i)\rho^{(P)}(\mathbf{R}) \tag{7}$$

where $\rho^{(P)}(\mathbf{R})$ is the local density of the chains and $\rho_{s,i}^{(P)}(\mathbf{r})$ is the density of the ith segments.

The second stage of calculations contains the minimization of the thermodynamic potential. In the considered system, the grafted density is fixed so that

$$\int_0^{(M+1/2)\sigma^{(P)}} dz\, \rho_{s,i}^{(P)}(z) = \rho_P \tag{8}$$

Under such a constraint, the thermodynamic potential is defined as

$$Y = F[\rho^{(P)}(\mathbf{R}), \rho^{(1)}(\mathbf{r}_1), \rho^{(2)}(\mathbf{r}_2)] + \int d\mathbf{R}\, \rho^{(P)}(\mathbf{R})v^{(P)}(\mathbf{R}) + \sum_{k=1,2} \int d\mathbf{r}_k\, \rho^{(k)}(\mathbf{r}_k)(v^{(k)}(\mathbf{r}_k) - \mu^{(k)}) \tag{9}$$

Finally, we solve numerically the set of the Euler−Lagrange equations (cf. eq 17 in ref 54) that follow from the minimization of the thermodynamic potential. This procedure gives the density profiles of all of the species. In our model, the density distributions vary only with distance from the surface, $\rho^{(k)} = \rho^{(k)}(z)$.

Next, we can evaluate the excess adsorption isotherms of individual components

$$\Gamma^{(k)} = \int (\rho^{(k)}(z) - \rho_b^{(k)})\, dz \tag{10}$$

and the total excess adsorption isotherm

$$\Gamma^{(F)} = \int (\rho^{(F)}(z) - \rho_b^{(F)})\, dz \tag{11}$$

where $\rho^{(F)} = \rho^{(1)} + \rho^{(2)}$ is the total local density of the fluid and $\rho_b^{(F)} = \rho_b^{(1)} + \rho_b^{(2)}$ is the bulk total density.

We focus our attention on adsorption from solutions. Because this process has a competitive character, we define the relative excess adsorption isotherms as

$$N_k^e = \int (x^{(k)}(z) - x_b^{(k)})\, dz \tag{12}$$

where $x^{(k)} = \rho^{(k)}/\rho^{(F)}$ is the local mole fraction of the kth component and $x_b^{(k)}$ is its value in the bulk phase.

In this work, we express the energy parameters, $\varepsilon^{(kl)}$, in units of thermal energy k_BT, that is, we define dimensionless quantities $\varepsilon^{(kl)} = \beta\bar{\varepsilon}^{(kl)}$ and $\varepsilon_s^{(k)} = \beta\bar{\varepsilon}_s^{(k)}$. Moreover, we assume that all of the segments of chains and spherical molecules have the same diameters, $\sigma^{(k)} = \sigma$ ($k = P, 1, 2$), and take σ as the unit of the length.

3. RESULTS AND DISCUSSION

The density functional theory outlined above has been developed for a specific model and involves several approximations. However, even in the case of real experimental setups that mimic all of the assumptions of the theory, its application to measured adsorption data would require optimization of numerous parameters entering the final equations. Therefore, the purpose of our research is not to fit experimental adsorption isotherms but to carry out model calculations with the aim of reproduction of experimental observations at a qualitative level. To do that, we will vary in a systematic way selected parameters in order to study how those changes affect adsorption isotherms. Our interest is in the determination of the effect of the grafting density, the length of grafted chains, the interactions between different species in the liquid phase, as well as the interactions of the fluid molecules with the surface upon the competitive adsorption of components of a binary liquid mixture. In contradiction to phenomenological approaches,[10−12] the presented method gives also insight into the structure of the interface layer.

Our calculations have been carried out for a model surface that mimics the surface of a polar adsorbent (e .g., a silica gel surface) modified by tethered alkyl-like chains. The total bulk density of a binary liquid mixture is fixed and corresponds to a model aqueous−organic mixture, $\rho_b^{(F)} = 0.8$. According to the model, the affinity of a component l to the substrate is altered by adjusting the energy parameter $\varepsilon_s^{(l)}$, while its affinity to the tethered chains, by changing the value of $\varepsilon^{(Pl)}$. component 1 has a high affinity to the grafted chains but a relatively weak affinity to the polar substrate. However, component 2 can mimic either an organic solvent or water, depending on the values of the parameters $\varepsilon^{(P2)}$ and $\varepsilon_s^{(2)}$. In both cases, the molecules of component 2 are assumed to be more strongly attracted to the bare surface than the molecules of component 1, that is, $\varepsilon_s^{(2)} > \varepsilon_s^{(1)}$. We consider two classes of mixtures. In the first case, the mixture contains two "organic" species, which interact with the grafted chains in a similar way. In the second case, we model aqueous solutions of an organic component 1; therefore, the affinities of both components of the mixture to the tethered chains are considerably different. Of course, depending on the values of the parameters $\varepsilon^{(kl)}$, $k,l = 1,2$, the bulk binary mixture can undergo demixing transitions. However, all of the model fluids under studied conditions exhibit a complete mixing in the bulk phase.

In order to limit the number of the parameters of the model to a minimum, our calculations have been performed by fixing the values of the following parameters: $\varepsilon^{(PP)} = \varepsilon^{(22)} = \varepsilon^{(12)} = 1$ and $\varepsilon_s^{(1)} = 1$. The values of the remaining parameters that characterize the interactions in the liquid phase, the interactions with tethered chains, and the interactions of component 2 with the solid surface, that is, the values of $\varepsilon^{(11)}$, $\varepsilon^{(P1)}$, $\varepsilon^{(P2)}$, as well as $\varepsilon_s^{(2)}$, are varied. All of the results presented below, except for those displayed in Figure 2b, have been obtained for tethered octamers, $M = 8$.

We begin with the discussion of the relative excess isotherms, compare eq 12, for selected model systems. In Figures 1−4, we show the relative excess isotherms of component 1. Our theoretical results can be compared with experimental data that were reported in the literature.[11−16]

Figure 1 illustrates the influence of the grafting density on the relative excess adsorption isotherms, N_1^e, for some selected mixtures composed of two organic species. Similar dependences, but obtained for "aqueous−organic" solutions, are displayed in Figure 2. In Figure 1, we show the results obtained for $\varepsilon_s^{(2)} = 6$ and for the model systems in which the affinity of the first component to the grafted chains is greater than the affinity of the second component, $\varepsilon^{(P1)} > \varepsilon^{(P2)}$. If attractive interactions between molecules 1 are weaker than their interactions with the brush, that is, $\varepsilon^{(11)} < \varepsilon^{(P1)}$, then an

dx.doi.org/10.1021/jp300114y | J. Phys. Chem. B 2012, 116, 3115−3124

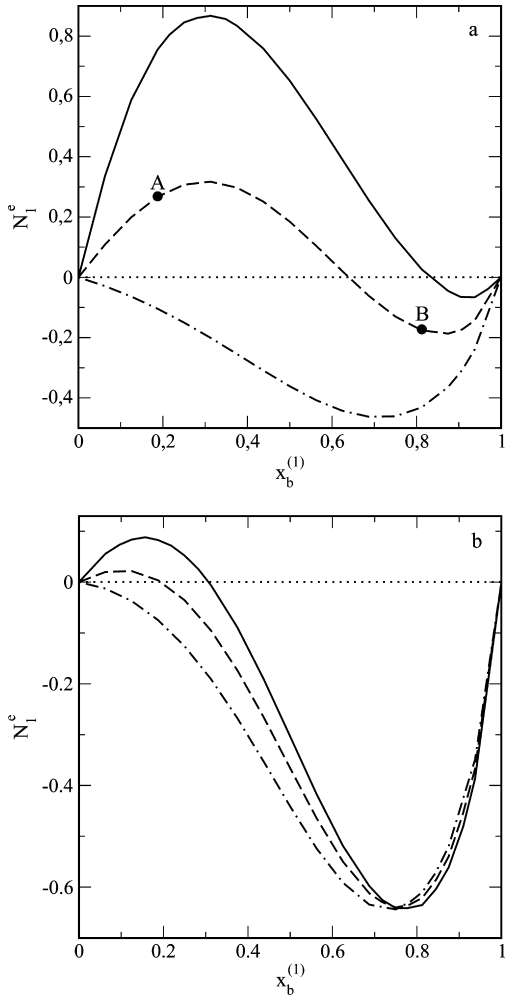

Figure 1. The dependence of the relative excess isotherms, N_1^e, on the density of grafted chains, ρ_P, built of $M = 8$ segments for mixtures composed of two organic-like species. The affinity of component 2 to the surface, $\varepsilon_s^{(2)} = 6$, is higher than the affinity of component 1, $\varepsilon_s^{(1)} = 1$. The affinity of component 2 to the chains, $\varepsilon^{(P2)} = 1.0$, however, is lower than the affinity of the first component. In panel (a), component 1 chains and component 1−component 1 interactions are characterized by $\varepsilon^{(P1)} = 1.2$ and $\varepsilon^{(11)} = 1.16$. Consecutive curves are for $\rho_P = 0.01$ (dotted−dashed line), 0.1 (dashed line), and 0.2 (solid line). In panel (b), we set $\varepsilon^{(P1)} = 1.1$ and $\varepsilon^{(11)} = 1.2$, and consecutive curves are for $\rho_P = 0.05$ (dotted−dashed line), 0.1 (dashed line), and 0.15 (solid line). The density profiles calculated at the points A and B are shown in Figure 7.

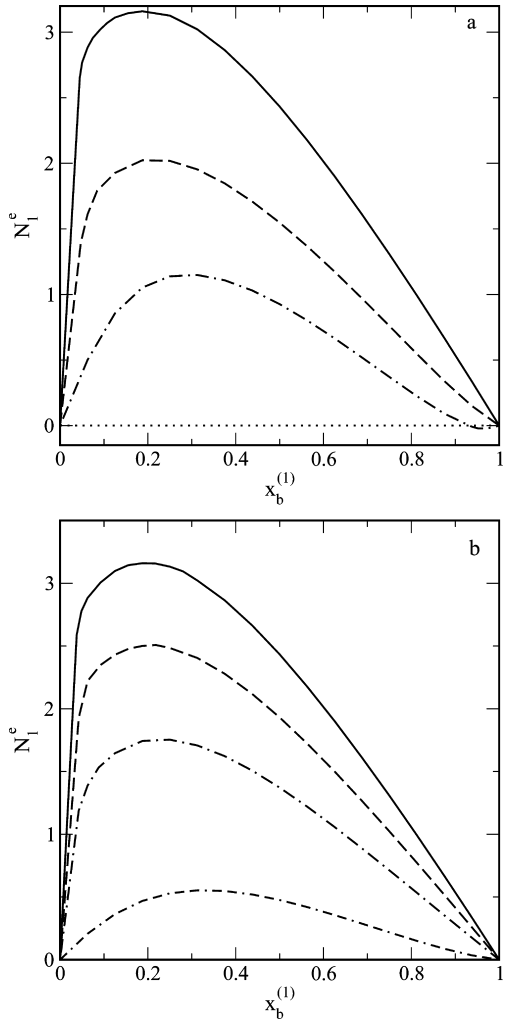

Figure 2. The dependence of the relative excess isotherms N_1^e on the grafting densities (a) and on the length of the chains part (b). The calculations are for organic−water mixtures; therefore, component 2 exhibits a very high affinity to the surface, $\varepsilon_s^{(2)} = 10.0$, and a very weak affinity to the chains, $\varepsilon^{(P2)} = 0.2$. The remaining energy parameters are $\varepsilon^{(P1)} = 1.2$ and $\varepsilon^{(11)} = 1.1$. The consecutive curves in (a) are for $M = 8$ and $\rho_P = 0.05$ (dotted−dashed line), 0.1 (dashed line), and 0.25 (the solid line). In panel (b), the grafting density is fixed, $\rho_P = 0.25$, and the number of segments is varied, $M = 2$ (dotted−double dashed line), 4 (dotted−dashed line), 6 (the dashed line), and 8 (solid line).

increase of the grafting density causes a significant increase of the relative excess adsorption N_1^e (see Figure 1a). Such a trend is observed in the experimental data.[14,16]

With an increase of the grafting density, the relative excess adsorption can even change from negative to positive. A similar effect, but taking place only for low concentrations $x_b^{(1)}$, is also observed when $\varepsilon^{(11)}$ is slightly greater than $\varepsilon^{(P1)}$ (see Figure 1b). In this case, the relative excess adsorption isotherms for different grafting densities cross together at $x_b^{(1)} \approx 0.75$. For high concentrations of component 1 in the bulk phase, its relative adsorption decreases slightly with increasing grafting density.

In Figure 1a and b, the adsorption azeotropy is observed. This means that for a certain composition of the liquid mixture, the relative excess adsorption equals 0, $N_1^e(x_{az}^{(1)}) = 0$ for $0 < x_{az}^{(1)} < 1$. The point $x_{az}^{(1)}$ is termed an azeotropic point.[63] At the azeotropic point, the relative excess adsorption isotherm changes sign. One can also say that at the azeotropic point, the composition of the surface layer is the same as the composition of the bulk solution. As shown in Figure 1, for denser brushes, the azeotropic point shifts toward higher concentrations of the first component.

The trends in the adsorption isotherms in Figure 1 are qualitatively consistent with predictions of simple theories of adsorption from binary solutions on solid surfaces.[18] These approaches forecast that adsorption azeotropy can occur if the difference between adsorption energies of two fluid components is not very large. The azeotropy can appear for nonideal solutions adsorbed on energetically homogeneous adsorbents and also for ideal liquid mixtures in contact with energetically heterogeneous surfaces. When, in the latter case, surface heterogeneity diminishes, the azeotropic point shifts toward the

dx.doi.org/10.1021/jp300114y | J. Phys. Chem. B 2012, 116, 3115−3124

mole fraction $x_b^{(1)} = 1$, and for a negligibly small heterogeneity, the adsorption azeotropy vanishes. The chemically modified surfaces behave like energetically heterogeneous adsorbents.[11,12] With an increase of the grafting density, the modified surface becomes effectively more energetically homogeneous.

In Figure 2, examples of the adsorption isotherms for a model organic solvent−water mixture are presented. To mimic such a system, we assume that the value of the energy parameter $\varepsilon_s^{(2)}$ is now much higher ($\varepsilon_s^{(2)} = 10$) than that in previous calculations (Figure 1). The relative excess adsorptions are plotted for different grafting densities (panel) and for different lengths of grafted chains (panel b).

In the considered case of an organic solvent−water mixture, the adsorption azeotropy occurs only for very low grafting densities, that is, when the role of the interactions of fluid components with the grafted chains is small (cf. dashed−dotted line in Figure 2a). Moreover, the azeotropic point appears at a high concentration of the organic solvent, $x_{az}^{(1)} \approx 0.93$. One can find similar results in the literature.[14]

Our theoretical predictions agree with experimental observations.[12−16] One can mention, for example, the adsorption of alcohols, acetonitrile, and tetrahydrofuran from water on end-capped C_{18} silica.[13] An increase of the grafting density causes an increase of the relative adsorption of acettonitrile and tetrahydrofuran in the whole concentration region. Moreover, as the surface coverage increases, the azeopropic points shift toward higher concentrations of the organic modifiers. The situation is different for methanol, ethanol, and 2-propanol. Again, for the bulk solutions rich in water, the relative excess adsorption of the organic component increases with increasing grafting density. However, the isotherms measured for different grafting densities cross together, and for higher concentrations of alcohols, the opposite effect is observed. Analogous results have also been reported for adsorption on the non-end-capped C_{18}-bonded phases.[14]

The impact of the chain length on the relative adsorption N_1^e is shown in Figure 2b. At a fixed grafting density, the relative excess adsorption of the organic component 1, N_1^e, becomes higher when the length of the chains increases. This is because in the system in question, the adsorption of molecules 1 results mainly from profitable contacts with the polymer segments. A similar trend has been observed for adsorption of methanol, acetonitrile, and tetrahydrofuran from water on the C_1−C_6, C_8, C_{10}, C_{12}, and C_{18} monomeric phases bonded to silica.[12]

One can conclude from the above discussion that interactions of both components, either with the underlying solid substrate or with the grafted chains, play a key role in the adsorption process. Figure 3 shows the influence of interactions with the substrate (panel a) and with the grafted chains (panel b) on the relative adsorption of the first component. These results have been obtained at fixed grafting density, $\rho_P = 0.15$, and for fixed values of the parameter $\varepsilon^{(11)} = 1.16$. In panel (a), we have also fixed the energy parameter $\varepsilon^{(P1)} = 1$ and varied the parameter $\varepsilon_s^{(2)}$ that characterizes interactions of the molecules 2 with the solid surface. The excess adsorption isotherm of the first component, N_1^e, decreases as the energy $\varepsilon^{(P2)}$ increases due to dispatchment of the molecules 1 by the molecules 2 in the surface layer. When the difference $\Delta = \varepsilon_s^{(2)} - \varepsilon_s^{(1)}$ increases, the azeotropic point shifts to the values of $x_b^{(1)}$ closer to unity. This observation is in accordance with numerous theoretical and experimental results obtained for adsorption on heterogeneous surfaces.[18]

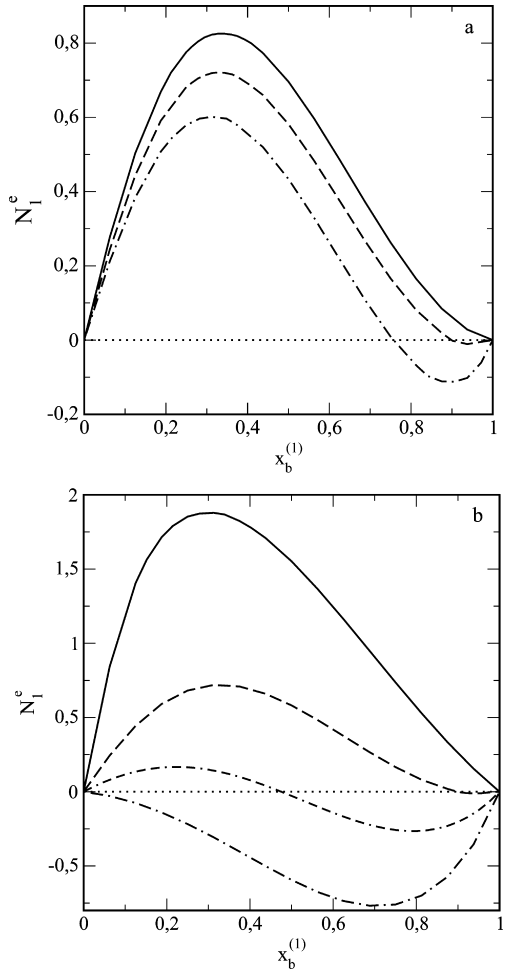

Figure 3. Relative excess isotherms N_1^e for different interactions of the second component of a mixture of two organic species with the bare surface (a) and of the first component with the grafted chains (b). In all cases, we fix the grafting density, $\rho_P = 0.15$, and the interaction parameters, $\varepsilon^{(P2)} = 1.0$ and $\varepsilon^{(11)} = 1.16$. In panel (a), the energy parameter $\varepsilon^{(P1)}$ is fixed, $\varepsilon^{(P1)} = 1.2$, but $\varepsilon_s^{(2)}$ is varied: $\varepsilon_s^{(2)} = 6.0$ (dotted−dashed line), 3.0 (dashed line), and 1.0 (solid line). In panel (b), the interactions of component 2 with the surface are kept constant, $\varepsilon_s^{(2)} = 1.0$, and the parameter $\varepsilon^{(P1)}$ is changed: $\varepsilon^{(P1)} = 1.0$ (dotted−dashed line), 1.1 (dotted−double dashed line), 1.2 (dashed line), and 1.4 (solid line).

Next, the calculations have been carried out by keeping the value of $\varepsilon_s^{(2)} = 6$ constant and changing the energy parameter $\varepsilon^{(P1)}$ that alters interactions of molecules 1 with the segments of grafted chains. The excess adsorption N_1^e reflects competition in the accumulation of components 1 and 2 of the fluid within the surface layer. Therefore, an increase of the energy parameter $\varepsilon^{(P1)}$ should have an effect similar to a decrease of the energy $\varepsilon_s^{(2)}$. This is illustrated in Figure 3b. A change of the parameters characterizing interactions with the brush segments causes a large change of the relative adsorption excess. If $\varepsilon^{(P1)}$ is the same as $\varepsilon^{(P2)}$ and $\varepsilon^{(P1)} = \varepsilon^{(P2)} = 1$, the excess relative adsorption is negative in the entire range of the mole fractions $x_b^{(1)}$. For $\varepsilon^{(P1)} = 1.4$, the values of N_1^e are positive and large. However, for $\varepsilon^{(P1)} = 1.1$ and 1.2, the adsorption azeotropy is observed. In the case of a lower value of $\varepsilon^{(P1)} = 1.1$, the azeotropic point is found at a moderate value of the mole fraction, $x_b^{(1)} = x_{az}^{(1)} \approx 0.48$. For $\varepsilon^{(P1)} = 1.2$, the azeotropic point appears at a quite high value of $x_b^{(1)} \approx 0.9$.

dx.doi.org/10.1021/jp300114y | J. Phys. Chem. B 2012, 116, 3115−3124

Finally, we have performed model calculations altering the interaction between the species 1, $\varepsilon^{(11)}$, and keeping all remaining parameters constant. The results are displayed in Figure 4. If $\varepsilon^{(11)}$ is large enough, the molecules of component 1

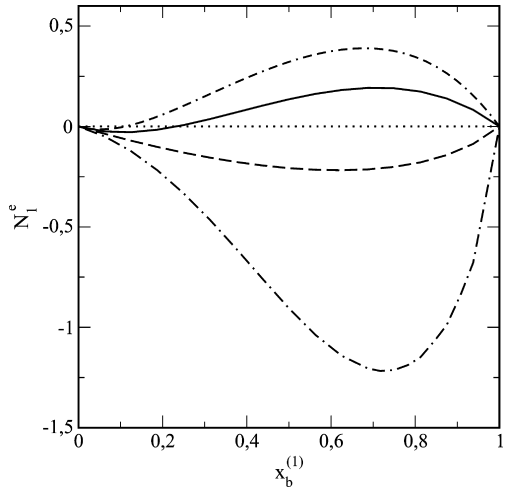

Figure 4. Relative excess isotherms N_1^e for different interactions between molecules of component 1: $\varepsilon^{(11)}$ = 1.2 (dotted−dashed line), 1.0 (dashed line), 0.8 (solid line), and 0.6 (dotted−double dashed line). The values of the remaining parameters are $\varepsilon_s^{(2)}$ = 6, $\varepsilon^{(P1)}$ = 1, $\varepsilon^{(P2)}$ = 1, and ρ_P = 0.15.

are "sucked" into the bulk phase, and their concentration within the surface layer decreases. Consequently, N_1^e is negative for all bulk-phase concentrations $x_b^{(1)}$. For lower values of $\varepsilon^{(11)}$ = 0.8, the adsorption isotherm N_1^e changes its sign from negative at low bulk concentrations to positive at higher concentrations. The azeotropic point appears at a low value of $x_{az}^{(1)} \approx 0.25$. When $\varepsilon^{(11)}$ becomes still lower and $\varepsilon^{(11)}$ = 0.6, the azeotropic point shifts to lower values of the mole fraction of the first component, $x_{az}^{(1)} \approx 0.11$.

The relative excess adsorption N_1^e results from an interplay between various attractive interactions and the entropic repulsion in the system. Moreover, the competitive adsorption N_1^e is very sensitive to even small changes of thermodynamic conditions. Therefore, it is difficult to predict the shape of the relative excess isotherm for a chosen set of system parameters.

For a better understanding of the adsorption mechanism, one needs to know the structure of the surface region. In the literature concerning adsorption on solid surfaces covered by grafted chains, three types of adsorption have been distinguished. The adsorption process can occur (i) directly at the solid surface (the so-called primary adsorption), (ii) at the outer edge of the bonded phase (secondary adsorption), and (iii) from confinement of fluid molecules within the brush (ternary adsorption).[64] The ternary adsorption is often treated as partitioning molecules between the bonded phase and the bulk phase[3] or as absorption inside of the polymer film.[55] Which adsorption effect prevails, primary, secondary, or ternary, depends on the nature of fluid molecules and that of the modified adsorbent, that is, on the parameters of the model. The above question can be answered by analyzing the density profiles of fluid species and grafted chains.

In Figure 5, we show the total segment density profiles of the grafted chains, while Figure 6 presents examples of the profiles of both components. The calculations are for the systems from Figure 1a. We recall that Figure 1a displayed the relative excess

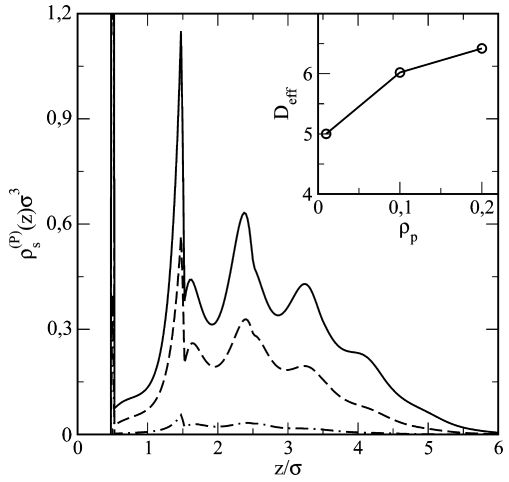

Figure 5. Segment density profiles of tethered chains for different grafting densities: ρ_P = 0.01 (dotted−dashed line), 0.1 (dashed line), and 0.2 (solid line). The calculations are performed for the same parameters as those in Figure 1a, assuming $\rho_b^{(1)}$ = 0.15. The inset shows the dependence of the effective brush height on the grafting density.

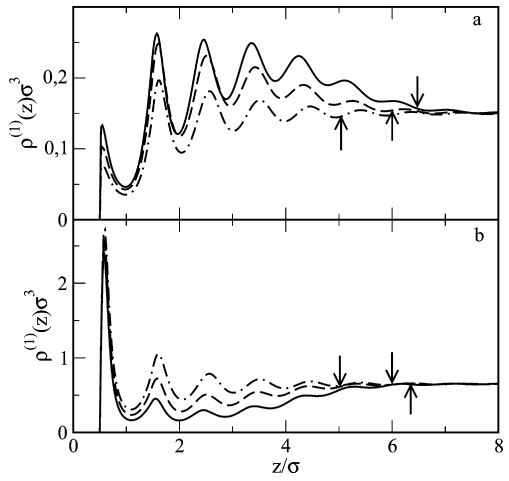

Figure 6. Density profiles of components 1 (a) and 2 (b) for different grafting densities: ρ_P = 0.01 (dotted−dashed line), 0.1 (dashed line), and 0.2 (solid line). The calculations are performed for the same parameters as those in Figure 1a, assuming $\rho_b^{(1)}$ = 0.15. Arrows indicate the position of the brush edge.

adsorption isotherms for the binary mixture of organic-like species. The calculations have been performed for the bulk densities $\rho_b^{(1)}$ = 0.15 and $\rho_b^{(2)}$ = 0.65. The mole fraction of the first component in the bulk mixture is relatively low, namely, $x_b^{(1)}$ = 0.1875. Close to the surface, the total segment density profiles exhibit a liquid-like structure with peaks corresponding to five consecutive layers of polymer segments. These peaks are followed by an extended tail region, in which the segment density smoothly decreases to zero. A simple parameter that can be used to describe the bonded phase is the effective height of the brush, D_{eff}, which is defined as the length of the region where the density of bonded chains is greater than zero. The maximum brush height equals $D_{max} = (M + 0.5)\sigma^{(P)}$. The effective brush height increases strongly with increasing density of the bonded phase. The positions of brush edges are indicated by arrows on the fluid density profiles.

dx.doi.org/10.1021/jp300114y | J. Phys. Chem. B 2012, 116, 3115−3124

The local densities of both components of the liquid mixture are shown in Figure 6a (the local densities of the molecules 1) and b (the profiles of the molecules 2). Note that both components are quite strongly attracted by the grafted chains. For this reason, both solvent species penetrate the brush well, provided that the density of the brush is not too high. The positions of the local density peaks of the two solvent species are correlated with the positions of the density peaks of the grafted chains (cf. Figure 5). One can even say that the solvent molecules "stick" to the tethered polymers. However, the molecules of components 1 and 2 are differently distributed within the surface layer. In the case of component 1, the height of the local density peak adjacent to the solid surface is significantly lower than the height of the consecutive peaks and even lower than the bulk density of that component. On the contrary, for component 2, the maximum of the first peak is higher than the height of all of the remaining peaks and higher than the bulk density. This is due to stronger interactions of the molecules of component 2 with the surface than that of the molecules of component 1.

The structure of a middle part of the bonded phase depends on the grafting density. A denser bonded phase offers more energetically profitable "contacts" with the molecules 1; therefore, an increase of the grafting density enhances the ternary adsorption of this solvent. An opposite trend is observed for component 2. For $\rho_P = 0.1$ and 0.2, the densities of component 2 in the interior of the brush are lower than those in the bulk mixture. There is also the secondary adsorption of the molecules 1 atop the brush. In the interfacial region, the solvent densities tend gradually to the bulk values.

Summing up, in the systems shown in Figure 6, one can see a considerable enrichment in the concentration of component 1 in the whole surface region. The density of component 1 reaches a maximum in the middle part of the bonded phase, whereas the density of component 2 is the highest near the surface. It should be mentioned, however, that for sufficiently dense brushes, the excluded volume effects cause a depletion of the total solvent density in the surface region ($\rho^{(F)} < \rho_b^{(F)}$).[51−54]

The structure of the surface layer depends also on the composition of the bulk mixture. These effects are shown in Figure 7. The density profiles presented here have been calculated at points A and B, which have been marked in Figure 1a. The bulk composition at point A, $x_b^{(1)} = 0.1875$, is lower than that at the azeotropic point. The relative excess adsorption N_1^e is positive. In this case, the density of the first component (solid line) is always lower than the density of the second component (dotted−dashed line), $\rho^{(1)}(z) < \rho^{(2)}(z)$. However, at point B, at which the bulk composition, $x_b^{(1)} = 0.8125$, is higher than that at the azeotropic point, the relative excess adsorption N_1^e is negative. Now, the relation between the densities of components is inverted in the almost whole system, namely, $\rho^{(1)}(z) > \rho^{(2)}(z)$ for $z > 0.88$. In the vicinity of the wall, this relation changes and again $\rho^{(1)}(z) < \rho^{(2)}(z)$. The primary adsorption of the molecules 2 (dotted line) is considerably greater than that for the molecules 1 (dashed line). Despite these differences, the total density profiles of the fluid at points A and B are very similar (see Figure 7b). As a consequence, the total density profiles of the segments depend only slightly on the bulk-phase concentration. Nevertheless, we observe that the profile $\rho_s^{(P)}(z)$ evaluated at point B is more "smeared out" than the profile at point A. Because the bulk density is the same in both systems, this difference is due to different attraction of species 1 and 2 with the segments of the chains and with the wall. We conclude that for components having comparable affinities to the tethered chains, an influence of the mixture composition on the brush structure is rather weak. Because the bulk density is the same in both systems, this difference is due to different attraction of species 1 and 2 with the segments of the chains and with the wall.

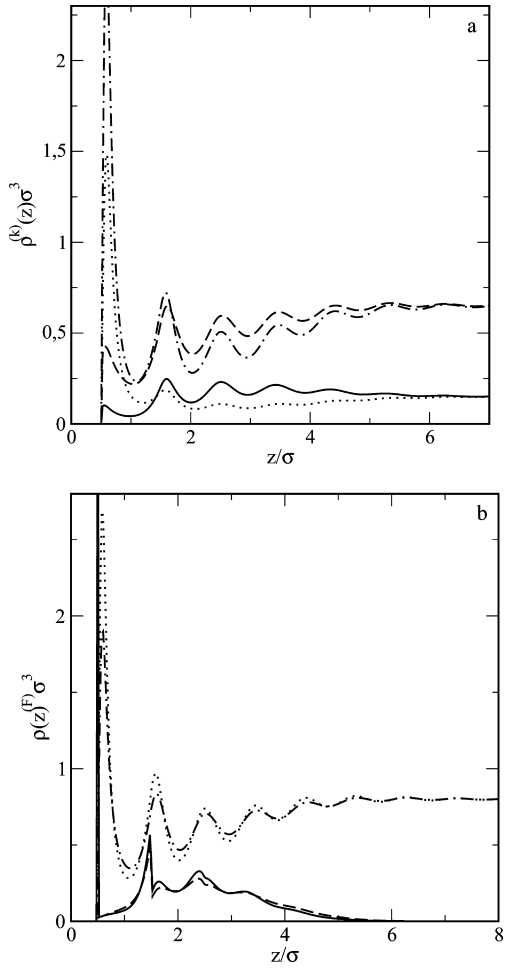

Figure 7. Density profiles of components 1 and 2 (a) and total density profiles of the fluid, $\rho^{(F)} = \rho^{(1)} + \rho^{(2)}$ and segment profiles of the tethered chains at points A and B that have been marked in Figure 1a. The points A and B are at $x_b^{(1)} = 0.1875$ and 0.8125, respectively. The grafting density is $\rho_P = 0.15$. All of the parameters are the same as those in Figure 1a. The curves are marked as follows. (a) Density profiles at point A: for components 1 (solid line) and 2 (dotted−dashed line); the density profiles at point B: for components 1 (solid line) and 2 (dotted−dashed line); (b) the density profile of the fluid (dotted−dashed line) and the segment density profile of the grafted chains (solid line) at point A; the density profile of the fluid (dotted line) and the segment density profile of the grafted chains (dashed line) at point B.

Now, we consider the structure of the surface layer in the case of a model "aqueous solution". The profiles in Figures 8 and 9 correspond to the excess adsorption isotherm that is displayed as a solid line in Figure 2a. Figure 8 shows the total segment density profiles, whereas Figure 9 presents the local densities of the particular components and the total density of the fluid. We recall that in the considered case, the grafting density is $\rho_P = 0.25$. Component 2, representing water, exhibits very high affinity to the surface, $\varepsilon_s^{(2)} = 10.0$, and a very weak affinity to the chains, $\varepsilon^{(P2)} = 0.2$. In contrast, the affinity of

dx.doi.org/10.1021/jp300114y | J. Phys. Chem. B 2012, 116, 3115−3124

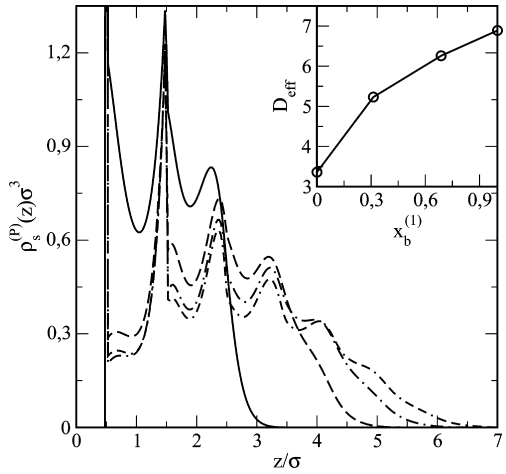

Figure 8. Segment density profiles of tethered chains for different mole fractions of component 1, representing an organic component. The calculations are for $x_b^{(1)} = 0$ (solid lines), 0.3125 (dashed lines), 0.6875 (dotted−dashed lines), and 1.0 (dotted-double dashed lines). The grafting density is $\rho_P = 0.25$. The remaining parameters are the same as those in Figure 2a. The inset shows the dependence of the effective brush height on the mole fraction of component 1.

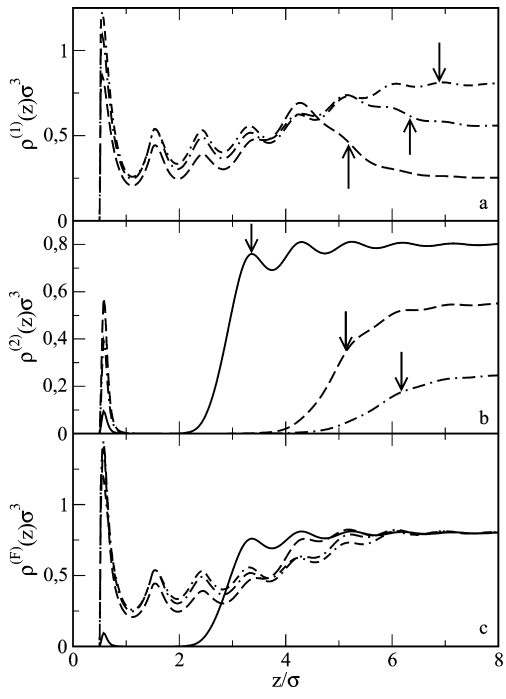

Figure 9. Density profiles of component 1 (a), density profiles of component 2 (b), and density profiles of the fluid $\rho^{(F)} = \rho^{(1)} + \rho^{(2)}$ (c) for different mole fractions of component 1: $x_b^{(1)} = 0.0$ (solid line), 0.3125 (dashed lines), 0.6875 (dotted−dashed lines), and 1.0 (the dotted−double dashed line). The grafting density is $\rho_P = 0.25$. The remaining parameters are the same as those in Figure 2a. Arrows indicate the position of the brush edge.

component 1 (an organic component) to the chains is high, $\varepsilon^{(P1)} = 1.2$. Therefore, for $x_b^{(1)} = 0$, the solvent is poor, while for $x_b^{(1)} = 1$, it is good with respect to the chains.

For $x_b^{(1)} = 0$, the bonded brush forms a quite compact layer (cf. Figure 8). This structure is typical for an intermediate density brush in contact with a bad solvent. When the concentration of the organic component increases, the grafted chains become more stretched. Indeed, with an increase of $x_b^{(1)}$, the solvent becomes "better", and the fluid molecule of component 1 that enters the brush interior (cf. Figure 9a) pushes the brush segments away from the surface. This effect is also reflected by the increasing effective height of the tethered layer; compare the inset to Figure 8. Note that similar trends have been also observed in computer simulations.[28,29]

Complementary to the density profiles of grafted chains, in Figure 9, we show the density profiles of the fluid components. We stress the difference between the shape of the profiles for mixtures of two organic solvents, which have already been presented in Figures 6 and 7, and the profiles for components of aqueous solutions in Figure 9. Although, similar to previous cases, the molecules of the organic component 1 solvate the grafted chains, the molecules of component 2 (representing water) are absent in the interior of the bonded phase, except for a small peak at the wall. Despite of a large value of $\varepsilon_s^{(2)}$, the height of this local density maximum is small. In fact, it is even lower than the height of the corresponding maximum of the local density of component 1, though the interaction of the latter component with the wall is significantly lower. This can be explained by the following effects. The surface density of the pinned segments is appreciably high, and these segments strongly attract the molecules of component 1. A high density of the pinned segments and molecules of component 1 stuck to them delimits the space accessible for the adsorption of component 2. We also stress a nonmonotonic changes of the height of the first local density peak $\rho_s^{(2)}(z)$ with $x_b^{(1)}$. This peak is the lowest for $x_s^{(1)} = 0$. However, for that system, the density of the brush in the surface vicinity is very high, which prohibits the adsorption of component 2. With the $x_b^{(1)}$ increase, the brush becomes less compact, which allows the molecules 2 to enter the surface region. An interplay between volume exclusion and attraction effects results in a nonmonotonic behavior of the height of local density $\rho_s^{(2)}(z)$ maximum at the wall.

In Figure 9c, the total fluid density profiles ($\rho^{(F)}$) are shown. As there is more organic component in the mixture, its penetration into the interior of the polymer film is stronger. The opposite trend is observed in the outer region of the surface phase.

Figure 10 presents the total density profiles ($\rho = \rho^{(F)} + \rho^{(P)}$) plotted for the systems shown in Figure 9. An interesting phenomena is found for the pure water-like component 2. In the interfacial region between the bonded phase and the bulk solvent, the total density is lower than that in the bulk part of the system. The computer simulations by Zhang et. al[28] show such minima in the total densities calculated for water and the water-rich mixtures. In our model system, however, addition of component 1 causes this effect to diminish.

It follows from the above discussion that adsorption from solution on chemically bonded phases is a very complex phenomenon that depends on numerous parameters. However, the application of the density functional theory allows modeling of this process for a wide spectrum of real systems.

4. SUMMARY

We have studied adsorption of binary solutions on solid surfaces modified with grafted chains using the density functional theory. We have assumed that solution molecules are spherical. The free molecules as well as segments of grafted chains interact via Lennard-Jones (12−6) potentials. All segments of tethered polymers but the surface-binding segment

dx.doi.org/10.1021/jp300114y | J. Phys. Chem. B 2012, 116, 3115−3124

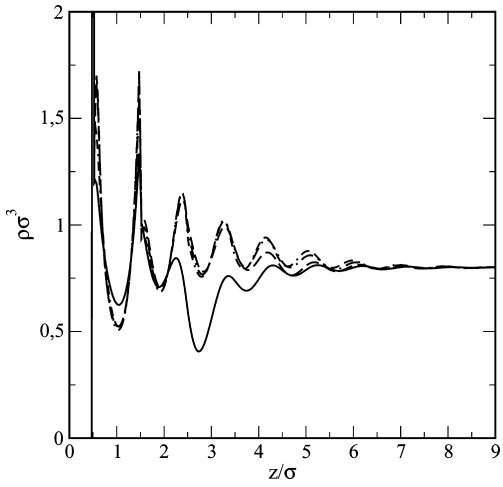

Figure 10. Total density profiles, $\rho = \rho^{(P)} + \rho^{(F)}$, for for different mole fractions of component 1: $x_b^{(1)} = 0.0$ (solid line), 0.3125 (dashed lines), 0.6875 (dotted−dashed lines), and 1.0 (dotted−double dashed line). The grafting density is $\rho_P = 0.25$. The remaining parameters are the same as those as in Figure 2a. Arrows indicate the position of the brush edge.

are neutral with respect to the substrate. The fluid molecules are attracted by the wall via the Lennard-Jones (9−3) potential. The study has shown that adsorption of mixture components depends on their properties and the nature of the whole adsorbing material, that is, the substrate and the bonded phase. An equilibrium is the result of complex interplay between two fundamental factors, the attractive interactions in the system and the entropic repulsion in the film built of tethered chains. We have systematically discerned the effect of various parameters on the adsorption from solutions and the structure of the surface layer. We have examined the role of the grafting density, the length of grafted chains, the strength of interactions with the substrate and with the grafted chains, the quality of solvent, and its composition. This is the first application of the density functional theory to study adsorption from binary solutions on the bonded phases.

We have shown how different parameters affect the relative excess isotherm. Because both components compete for space inside of the bonded phase, the resulting relative excess adsorption isotherms may be different depending on relations between various parameters. The adsorption azeotropy has been found for selected systems. An influence of the grafting density on the position of the azeotropic point has been analyzed.

We have performed calculations for two classes of the liquid mixtures, namely, the mixtures of two organic solvents and mixtures that mimic aqueous solutions of organic solvents. The most important observation from the study is that the surface region is highly inhomogeneous, and its structure depends strongly on a type of solution. In the case of the organic mixture, both components penetrate the polymer film in a similar way. However, for aqueous solutions, the qualitative difference in the behavior of components is observed. The component that mimics water is practically absent in the interior of the bonded phase. As the mole fraction of the organic solvent increases, there is a considerable increase in the degree of solvent penetration into the bonded phase.

The structure of the polymer brush is strongly affected by the grafting density and the composition of the bulk solution. The effective height of the brush increases with increasing the grafting density and the concentration of the less polar solvent. As the structure of the brush changes, the structure of the interfacial region between the surface region and the bulk solution also varies.

The density functional theory provides a description of adsorption from binary solution on surfaces modified with grafting chains. The results of the theoretical predictions are consistent with experimental observations and the conclusions following from computer simulations.

AUTHOR INFORMATION

Corresponding Author

*E-mail: tomo@heksan.umcs.lublin.pl.

Notes

The authors declare no competing financial interest.

ACKNOWLEDGMENTS

This work was supported by the Ministry of Science and Higher Education of Poland under Grant No. N N204 151237 (S.S.) and by EC under Grant No. PIRSES-GA2010-268498 (M.B.).

REFERENCES

(1) Martire, D. E.; Boehm, R. E. *J. Phys. Chem.* **1983**, *87*, 1045.
(2) Dill, A. K. *J. Phys. Chem.* **1987**, *91*, 1980.
(3) Dorsey, J. G.; Dill, A. K. *Chem. Rev.* **1989**, *89*, 331.
(4) Bohmer, M. R.; Koopal, L. K.; Tijssen, R. *J. Phys. Chem.* **1991**, *92*, 6285.
(5) Tijssen, R.; Schoenmakers, P. J.; Bohmer, M. R.; Koopal, L. K.; Boliet, H. A. H. *J. Chromatogr., A* **1993**, *656*, 135.
(6) Sentell, K. B.; Dorsey, J. G. *Anal. Chem.* **1989**, *61*, 930.
(7) Boehm, R. E.; Martire, D. E. *J. Phys. Chem.* **1994**, *98*, 1317.
(8) Tan, L. C.; Carr, P. W. *J. Chromatogr., A* **1997**, *775*, 1.
(9) Bórowko, M; Ościk-Mendyk, B.; Bórowko, P. *J. Phys. Chem. B* **2005**, *109*, 21056.
(10) Jaroniec, M. *J. Chromatogr., A* **1993**, *656*, 37.
(11) Gritti, F.; Guiochon, G. *J. Chromatogr., A* **2007**, *1155*, 85.
(12) Kazakevich, Y. V.; LoBrutto, R.; Chan, F.; Patel, T. *J. Chromatogr., A* **2001**, *913*, 75.
(13) Gritti, F.; Kazakevich, Y. V.; Guiochon, G. *J. Chromatogr., A* **2007**, *1169*, 111.
(14) Bocian, S.; Vajda, P.; Felinger, A.; Buszewski, B. *Anal. Chem.* **2009**, *81*, 6334.
(15) Bocian, S.; Vajda, P.; Felinger, A.; Buszewski, B. *Chromatography* **2010**, *71*, S5.
(16) Buszewski, B.; Bocian, S.; Rychlicki, G.; Vajda, P.; Felinger, A. *J. Colloid Interface Sci.* **2010**, *349*, 620.
(17) Bórowko, M.; Jaroniec, M. *Adv. Colloid Interface Sci.* **1983**, *19*, 137.
(18) Bórowko, M *Adsorption, Theory, Modeling, and Analysis*; Surfactant Science Series; Toth, J., Ed.; M. Dekker: New York, 2002; v.107, Chapter 2.
(19) Klatte, S. J.; Beck, T. L. *J. Phys. Chem.* **1993**, *97*, 5727.
(20) Klatte, S. J.; Beck, T. L. *J. Phys. Chem.* **1995**, *99*, 16024.
(21) Klatte, S. J.; Beck, T. L. *J. Phys. Chem.* **1996**, *100*, 5931.
(22) Yarovsky, I.; Aguilar, M. I.; Hearn, M. T. W. *Anal. Chem.* **1995**, *67*, 2145.
(23) Yarovsky, I.; Hearn, M. T. W.; Aguilar, M. I. *J. Phys. Chem. B* **1997**, *101*, 10962.
(24) Sluster, J. T.; Mountain, R. D. *J. Phys. Chem. B* **1999**, *103*, 1354.
(25) Lippa, K. A.; Sander, L. C.; Mountain, R. D. *Anal. Chem.* **2005**, *77*, 7852.
(26) Pastorino, C.; Binder, K.; Keer, T.; Mueller, M. *J. Chem. Phys.* **2006**, *124*, 064902.
(27) Ban, K.; Saito, Y.; Jinno, K. *Anal. Sci.* **2005**, *21*, 397.

(28) Zhang, L.; Rafferty, J. L.; Siepmann, I.; Chen, B.; Schure, M. R. *J. Chromatogr., A* **2006**, *1126*, 219.
(29) Rafferty, J. L.; Zhang, L.; Siepmann, I.; Schure, M. R. *Anal. Chem.* **2007**, *79*, 6551.
(30) Rafferty, J. L.; Siepmann, I.; Schure, M. R. *J. Chromatogr., A* **2008**, *1204*, 11.
(31) Rafferty, J. L.; Siepmann, I.; Schure, M. R. *J. Chromatogr., A* **2008**, *1204*, 20.
(32) Rafferty, J. L.; Siepmann, I.; Schure, M. R. *Anal. Chem.* **2008**, *80*, 6214.
(33) Rafferty, J. L.; Sun., L.; Siepmann, I.; Schure, M. R. *Fluid Phase Equilib.* **2010**, *290*, 25.
(34) Fouqueau, A.; Meuwly, M.; Bemish, R. J. *J. Phys. Chem. B* **2007**, *111*, 10208.
(35) Braun, J.; Fouqueau, A.; Bemish, R. J. *Phys. Chem. Chem. Phys.* **2008**, *10*, 4765.
(36) Alexander, S. *J. Phys. (France)* **1977**, *38*, 983.
(37) de Gennes, P. G. *Macromolecules* **1980**, *13*, 1069.
(38) Milner, S. T.; Witten, T. A.; Cates, M. E. *Europhys. Lett.* **1988**, *5*, 413.
(39) Milner, S. T.; Witten, T. A.; Cates, M. E. *Macromolecules* **1988**, *21*, 2610.
(40) Milner, S. T. *Science* **1991**, *251*, 905.
(41) Zhalina, E. B.; Borisov, O. V.; Pryamitsyn, V. A.; Birshtein, T. M. *Macromolecules* **1991**, *24*, 140.
(42) Fleer, G. J.: Cohen Stuart, M. A.; Scheutjens, J. M. H. M.; Cosgrove, T.; Vincent, B. *Polymers at Interfaces*; Chapman and Hall: London, 1993.
(43) Carignano, M. A.; Szleifer, I. *J. Chem. Phys.* **1994**, *100*, 3210.
(44) Carignano, M. A.; Szleifer, I. *Macromolecules* **1995**, *28*, 3197.
(45) Carignano, M. A.; Szleifer, I. *J. Chem. Phys.* **1995**, *102*, 8662.
(46) McCoy, J. D.; Teixeira, M. A.; Curro, J. G. J. *J. Chem. Phys.* **2002**, *117*, 2075.
(47) Ye, Y.; McCoy, J. D.; Curro, J. G. J. *J. Chem. Phys.* **2003**, *119*, 555.
(48) Cao, D. P.; Wu, J. *Langmuir* **2006**, *22*, 2712.
(49) Xu, X. F.; Cao, D. P. *J. Chem. Phys.* **2009**, *130*, 164901.
(50) Xu, X.; Cao, D. P. *Soft Matter* **2010**, *6*, 4631.
(51) Bórowko, M.; Rżysko, W.; Sokołowski, S.; Staszewski, T. *J. Chem. Phys. B* **2007**, *126*, 214703.
(52) Bórowko, M.; Rżysko, W.; Sokołowski, S.; Staszewski, T. *J. Phys. Chem. B* **2009**, *113*, 4763.
(53) Bórowko, M.; Sokołowski, S.; Staszewski, T. *J. Chromatogr., A* **2011**, *1218*, 711.
(54) Bórowko, M.; Sokołowski, S.; Staszewski, T. *J. Colloid Interface Sci.* **2011**, *356*, 267.
(55) Milchev, A.; Egorov, S. A.; Binder, K. *J. Chem. Phys.* **2010**, *132*, 184905.
(56) Yu, Y.-X; Wu, J. *J. Chem. Phys.* **2002**, *117*, 2368.
(57) Yu, Y.-X; Wu, J. *J. Chem. Phys.* **2002**, *117*, 10156.
(58) Yu, Y.-X; Wu, J. *J. Chem. Phys.* **2003**, *118*, 3835.
(59) Henderson, D., Ed.; *Fundamentals of Inhomogeneous Fluids*; M. Dekker: New York, 1992.
(60) Rosenfeld., J. *Phys. Rev. Lett.* **1989**, *63*, 980.
(61) Wertheim, M. S. *J. Chem. Phys.* **1987**, *87*, 7323.
(62) Weeks, J. D.; Chandler, D.; Andersen, H. C. *J. Chem. Phys.* **1971**, *54*, 5237.
(63) Everett, D. H. *Trans. Faraday Soc.* **1965**, *61*, 2478.
(64) Currie, E. P. K.; Norde, W.; Cohen Stuart, M. A. *Adv. Colloid Interface Sci.* **2003**, *100−102*, 205.